Journal of Applied Polymer Science

Effect of Hydration Layer on the Structure of Thermo-Sensitive Nanocapsules

Xianbo Xu, Guorong Shan, Yue Shang, Pengju Pan
State Key Laboratory of Chemical Engineering, Department of Chemical and Biochemical Engineering, Zhejiang University, Hangzhou 310027, China
Correspondence to: G. R. Shan (E-mail: shangr@zju.edu.cn)

ABSTRACT: A thermo-sensitive nanocapsule, containing the hydration layer, was synthesized through introducing *N*-isopropylacrylamide into the system of styrene miniemulsion polymerization and hexadecane as liquid template. The properties and content of the water in the hydration layer were investigated by differential scanning calorimetry. With dynamic light scattering and transmission electron microscope, the effects of temperature and solvent on the particle size and morphologies were studied. The results showed that the increase of temperature and the ethanol–water mixed solvent could decrease the thickness of hydration layer and caused the polymer chain in the shell coil-to-globule transition, which switched on the pathway to loading and releasing substances in the nanocapsules. By using UV-visible spectroscopy to monitor the tracer, the diffusion coefficients were determined and verified the switching process above. In addition, the ethanol–water molecule cluster can form a stable associative structure around ethanol mole fraction of 0.4, and destroyed the hydration of the hydrophilic group. The solvent interactions were proved to be the main driving force for the coil-to-globule transition of poly(*N*-isopropylacrylamide). Moreover, an appropriate latex particle size should exclude the hydration layer but stable dispersed in the solvent was suggested. © 2014 Wiley Periodicals, Inc. J. Appl. Polym. Sci. **2014**, *131*, 40589.

KEYWORDS: emulsion polymerization; lattices; morphology; nanoparticles; nanowires and nanocrystals

Received 4 December 2013; accepted 9 February 2014
DOI: 10.1002/app.40589

INTRODUCTION

Functional polymer nanocapsules with a core-shell structure have great applications in controlled drug delivery system, biochemical separation, biocarrier, and phase-change materials.[1–4] Thermo-sensitive polymers such as poly(*N*-isopropylacrylamide) (PNIPAM) will undergo a coil-to-globule transition in response to changes in temperature. It is well documented that PNIPAM solubility in water arises from the amide group forming hydrogen bonds with water and increasing the temperature above the lower critical solution temperature (LCST) causes a dehydration of the hydrophilic and hydrophobic moieties. The hydration has attracted much attention for its special interaction with polymer. The status and content of water in the polymer have demonstrated the significant effect on permeability and selectivity of polymer membrane.[5] A study of hydrogels identified that a specific coordinated water can bind the specific solutes selectively and changes the separation factor in aqueous solution.[6]

To date, most studies of the polymer hydration layer are focused on the macro-morphology as gel or membrane. Little is known about the latex particle in submicrometer size. Furthermore, the role of the water cluster structures in the coil-to-globule transition is few studied. To approach this dearth of research, it is essential to explore a novel feasible and effective method to identify the hydration layer of water-soluble polymer particles, and especially its impact on the permeation property of nanocapsules. In this study, we synthesized thermo-sensitive nanocapsules through introducing NIPAM into the system of styrene miniemulsion polymerization, using low molecular weight hydrocarbon as template.[7,8] The properties and thickness of the hydration layer were investigated. By means of ethanol–water mixture, the effect of solvent interactions on the polymer phase transition was studied. Moreover, the process of loading and releasing substances in the nanocapsules was monitored by ultraviolet-visible spectroscopy.

EXPERIMENTAL

Materials

Styrene (St, 99.5%) was washed with NaOH (10 wt %) aqueous solution and then further washed with distilled water until the washings became neutral. After it had been dried with anhydrous $MgSO_4$, the St was purified by vacuum distillation and kept in the refrigerator until use. γ-Methacryloxy propyl trimethoxysilane (γ-MPS, Aldrich) was used as received. *N*-isopropylacrylamide (NIPAM, Acros Organics) was purified by

recrystallization in *n*-hexane and then dried in a vacuum oven at room temperature. The crosslinker, divinylbenzene (DVB, Aldrich, 80%), was used as received. *n*-hexadecane (HD, 99%, Acros Organics) were used as hydrocarbon templates. Potassium persulfate (KPS, Acros organics) was used as initiator. Sodium dodecyl sulfate (SDS, 99%, Acros Organics), sodium bicarbonate were used as received. Deionized water was applied for all of the polymerization and treatment process.

Nanocapsule Synthesis

The typical procedure used to fabricate the thermo-sensitive nanocapsules was as follows. The oil-soluble monomer St (8.32 g), MPS (2.08 g), DVB (0.4 g), and NIPAM (0.8 g) were mixed with the hydrocarbon HD (10.8 g) to obtain the oil phase. This oil phase was added to the aqueous solution containing the surfactant SDS (0.216 g) and the pH buffer $NaHCO_3$ (0.2 g). The miniemulsion is prepared by ultrasonifying the mixture for 20 min using a pulsed sequence (10 s sonication followed by 5 s break) with a 560 W duty cycle (SCIENTZ, JY92) under magnetic agitation in an ice bath. The miniemulsion was then introduced into the jacketed reactor and purged with nitrogen. The temperature was raised to 70°C, and an aqueous solution of KPS (0.15 g) was fed into the reactor to start the polymerization. 30 min after the reaction initiated, an aqueous solution of NIPAM (0.8 g) was added dropwise with a Sp1001 syringe pump to the above miniemulsion over the course of 30 min. The polymerization was continued for 6 h under stirring at 300 rpm.

Characterization

The particle size and size distributions (as PDI) were measured by dynamic light scattering (DLS, Zetasizer 3000 HSA, Malvern) at different temperature. The PDI is a dimensionless number that describes the heterogeneity of the sample and it can range from 0 (monodisperse) to 1 (polydisperse). The nanocapsules were diluted in deionized water or ethanol–water mixture before analysis. Five measurements were performed and averaged for each sample.

Transmission electron microscopy (TEM) measurements were performed on a JEOL JSM-1230EXT2 microscope. The colloidal dispersions were diluted in water or ethanol and placed on a 400-mesh carbon-coated copper grid and air-dried.

Infrared spectra were recorded with a ThermoFisher Nicolet 5700 FTIR spectrometer. The difference spectra were obtained using the same samples saturated with water, air-dried to constant weight or vacuum freeze-dried.

Differential scanning calorimetry (TA DSC Q200) was used to measure the phase transition of water sorbed by the nanocapsules. After air-dried to constant weight, nanocapsules about l0 mg weight were heated in sealed capsules under nitrogen atmosphere. The DSC curves were obtained by heating from −40 to +50°C at a rate of 5°C/min. Cooling measurements were performed at the same rate from +50 to −40°C.

The cresol red, used as tracer, was diluted in water or ethanol to load in the high-speed centrifuged nanocapsules. The loading process at different temperature was studied by using ultraviolet–visible spectroscopy (SHIMADZU UV-1800) to monitor the tracer (the main absorption wavelength is at 429 nm). The same concentration of centrifuged nanocapsules diluted in water or ethanol were used as references. The nanocapsules, which had been loaded with cresol red to a balance in ethanol at 50°C, were rapidly cooled and then high-speed centrifugated to get nanocapsules containing the tracer. The precipitate was washed with solvent and diluted in water or ethanol at different temperature to study the releasing process by UV spectroscopy.

RESULTS AND DISCUSSION

Property and Content of the Hydration Layer

Water in polymer has been shown to exist in three status[9]: Nonfreezing water is water that has no detectable phase transition over the temperature range usually associated with the water freezing/melting transition from −73°C to 47°C; freezable bound water is the intermediate water having a phase transition temperature lower than 0°C; free freezing water is defined as the unbound water in the polymer having transition temperature, enthalpy, and shape of the DSC curves similar to those of pure water.

Water-polymer interactions are identified by FTIR (Figure 1). A distinct displacement towards low frequencies for air-dried sample was observed in the 3600–3000 cm^{-1} region [Figure 1(a)] for ν_{OH}(stretching), showing the difference between the bulk free water and water bound by polymer, which indicate the formation of a hydrogen bond between water and copolymer. When the copolymer contains more water, the 1600–1700 cm^{-1} region for amide carbonyl group [Figure 1(b)] was found to red shift to 1626 cm^{-1}, which is due to the increase of hydrogen bond with water. Meersman et al.[10] also observed the spectral changes in hydration properties and structure of PNIPAM by Fourier transform infrared. The IR peak of water in PNIPAM was at 3410 cm^{-1} instead of 3710 cm^{-1}, the peak frequency of free freezing water, demonstrating the intermolecular hydrogen bond with polymer.

Figure 2 shows the DSC heating and cooling curves for the nanocapsules air-dried to constant weight. Two freezing transitions were observed, suggesting the existence of two states of freezable water in nanocapsules, that is, peak A for free freezing water (transition at −1.51°C) having similar transition temperature with pure water, and peak B for freezable bound water (transition at −7.65°C). The peak C was for the phase transition of liquid core template HD.

The following factors were considered qualitatively: (i) the nonfreezing water is bonded to the hydrophilic group and surrounded by freezable water molecules, which have interaction with polymer as well as nonfreezing water, thus lead to a lower freezing/melting transition temperature; (ii) in addition to the hydration of hydrophilic group, the network structure of polymer was embedded with a part of free freezing water to reach equilibrium state with surroundings.[11] The content of equilibrium water (W_e, mass fraction) and freezable water (W_f) were determined from direct integration of the endothermic peaks. The content of nonfreezing water (W_n) was calculated by the eq. (1).

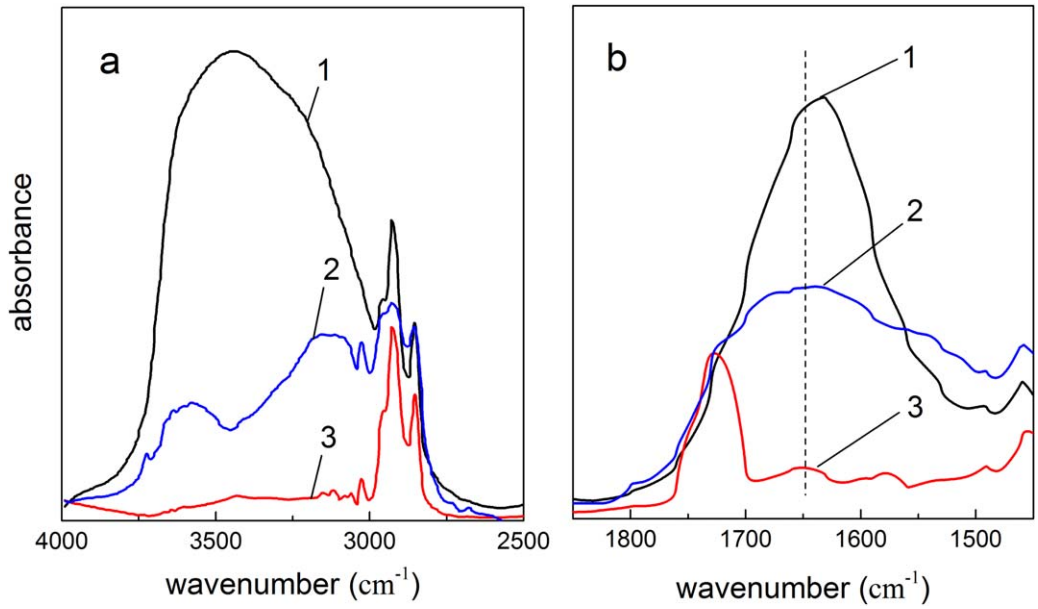

Figure 1. FTIR spectra of hybrid copolymers (1) saturated with water, (2) air-dried to constant weight, and (3) vacuum freeze-dried. [Color figure can be viewed in the online issue, which is available at wileyonlinelibrary.com.]

$$W_n = W_{\text{total}} - W_e - W_f \quad (1)$$

The content of total water in the specimen was defined as:

$$W_{\text{total}} = \frac{\text{weight of air dried emulsion} - \text{weight of emulsion} \times \text{solid content}}{\text{weight of air dried emulsion}} \quad (2)$$

where solid content include the content of monomer, HD, emulsifier and initiator, obtained by emulsion dried to constant weight at 150°C.

The computation results are shown in Table I.

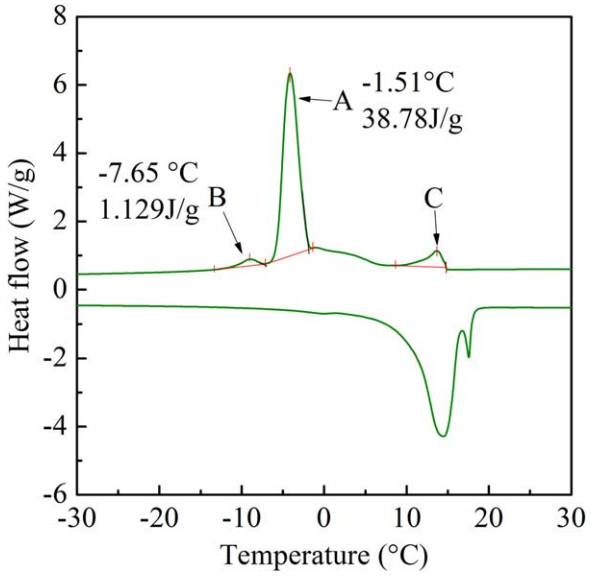

Figure 2. Differential scanning calorimetry curves of hybrid copolymers. [Color figure can be viewed in the online issue, which is available at wileyonlinelibrary.com.]

Effect of Temperature on the Hydration Layer

Water-soluble polymers like PNIPAM have hydrophilic groups to induce hydrogen bond with water, thus to form a certain thickness of hydration layer around the polymer particles. Since the PNIPAM chains undergo a coil-to-globule transition near its LCST, the particle size will change with the temperature variation.

The thermo-sensitivity of the synthesized nanocapsules was characterized by investigating the relationship between size and temperature. The Z-average size and particle size distribution of nanocapsules were showed in Table II and Figure 3, indicating that the size of nanocapsules decreased with the increase of temperatures. The PDI values decreased more obviously with increasing temperature, and the values are mainly less than 0.2, representing fairly narrow particle distribution.[12] A pronounced change of size with temperature takes place in the range of 35–40°C. The hydrogen-bond interaction between amide groups and water molecules, hydrophobic collapse and solvent-solvent interactions are considered to be the causes of coil-to-globule transition.[11,13] However, a computer simulation of the coil-to-globule collapse indicated that its dynamics is dominated by the solvent-induced interaction.[14]

Effect of Solvent on the Hydration Layer

The ethanol–water mixture is representative of the hydrogen-bond system. The solution structure behaviors, dynamic properties and polarity vary with concentration.[15] Therefore, the

Table I. Mass Fraction of Different Water Types

Different water types	W_e	W_f	W_n	W_{total}
Mass fraction (%)	11.63	0.34	0.46	12.43

Table II. Relationship Between Z-Average Size and Temperature

T (°C)	d_z (nm)[a]	PDI[b]
25	123.7 ± 0.6	0.216 ± 0.005
30	121.2 ± 0.5	0.195 ± 0.007
35	122.5 ± 1.1	0.186 ± 0.014
40	118.9 ± 0.9	0.169 ± 0.002
45	118.3 ± 0.7	0.155 ± 0.015
50	118.4 ± 1.0	0.123 ± 0.017

[a] The diameter was measured by DLS (5 mg/mL).
[b] PDI represents polydispersity index. The results are presented as means ± SD ($n = 5$).

relationship between the particle size and the concentration of ethanol was investigated to study the effect of solvent-induced interaction on the hydration layer.

Ethanol can make the hydrogen-bond structure of water more orderly at low concentrations ($x < 0.18$), thus to amplify the hydration layer.[16] The hydrogen-bond interaction between hydrophilic groups and water molecules was weakened by ethanol, for the water can form ethanol-associated clusters. With the mole fraction of ethanol increasing, the association between water and ethanol strengthened gradually. To a certain concentration of ethanol ($x = 0.08$), the water hydrogen-bond structure with hydrophilic groups had a balance with ethanol and the particle size attains maximum ($d_z = 184.0$ nm). When the concentration of ethanol was further increased, the water in polymer was "pulled out" by ethanol and form more stable clusters with ethanol. Therefore the thickness of hydration layer is gradually reduced, as well as the size of nanoparticles [Figure 4(a)]. The ethanol–water molecule cluster can form a rather stable associative structure around ethanol mole fraction of 0.4, and the mixed solvent was showing the lowest polarity. Thus, the hydrogen-bond interaction between polymer and water was the weakest and the thickness of hydration layer reached the minimum. Meanwhile the nanocapsules almost lost thermo-sensitivity d_z (25°C) = 95.0 nm, d_z (50°C) = 94.1 nm. This behavior were consistent with the results of Zhang et al.[17] They investigated the hydration and dynamic properties of ethanol–water mixtures at different ethanol mole fractions with molecular dynamics simulation, and the simulations indicated that the self-diffusion coefficient of water has a large drop at low concentrations of ethanol and then it nearly keeps constant, while the diffusion coefficient of ethanol has a minimum around ethanol mole fraction of 0.5. The partial molar volumes of ethanol–water solution were plotted in Figure 4(b).[18] As the partial molar volume of water reached the maximum at about $x = 0.1$, the affinity of ethanol–water was strongest and the hydrogen-bond structure between water molecules was the most orderly. It was obvious that the hydration layer of nanocapsules and particle size have the same variation trend with the partial molar volume of water, which proved that the solvent-induced interaction was the major driving force for the PNIPAM coil-to-globule transition.

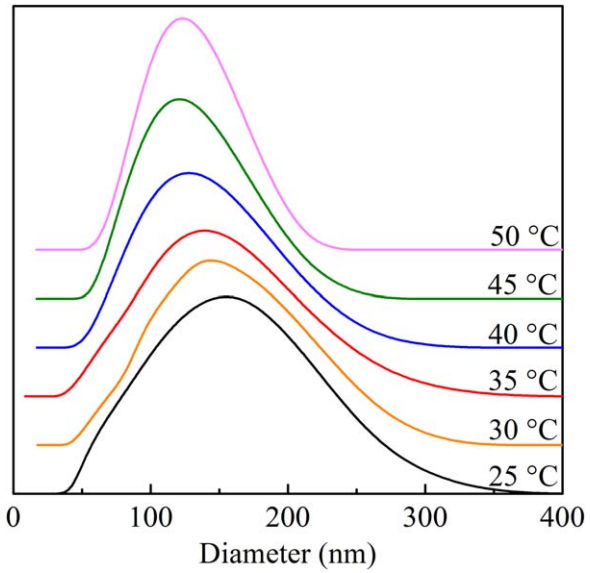

Figure 3. Z-average size and size distribution of nanocapsules at different temperatures. [Color figure can be viewed in the online issue, which is available at wileyonlinelibrary.com.]

Morphological Structure of Thermo-Sensitive Nanocapsules

Dynamic light scattering (DLS) has been widely used in the study about the size of polymer nanoparticles. However, the size investigated by DLS is the hydrodynamic diameter, including a certain hydration layer and much larger than the size in TEM, which is in the vacuum dry condition.

The TEM images of the synthesized nanocapsules [Figure 5(a)] showed the distinct core-shell structure of particles when the

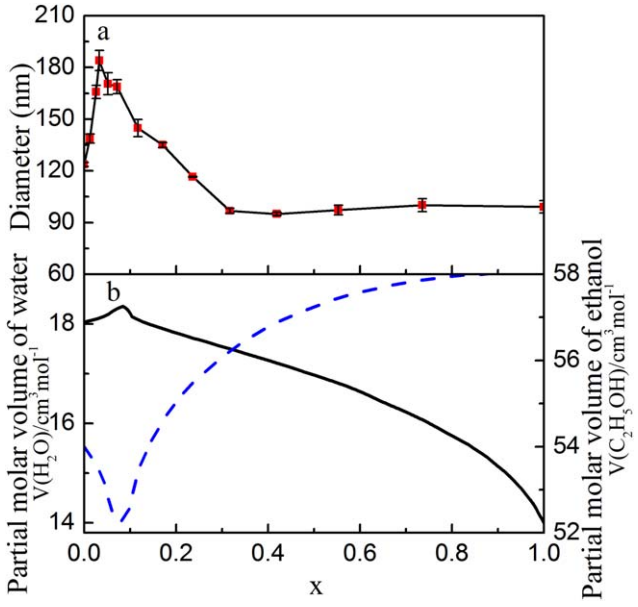

Figure 4. (a) Particle Z-average size of nanocapsules in the mixture of water-ethanol at 25°C, (b) The partial molar volumes of ethanol and water at 25°C.[18] Error bars indicate standard deviation for each sample. Where not shown, error bars are smaller than the data symbols. [Color figure can be viewed in the online issue, which is available at wileyonlinelibrary.com.]

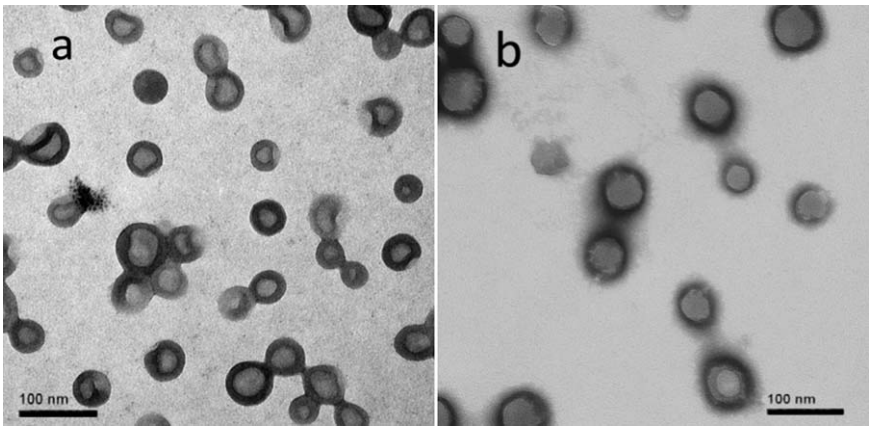

Figure 5. TEM image of nanocapsules (a) diluted in ethanol and dried at 50°C and (b) diluted in water and air dried at 25°C.

polymer chain was in aggregation state, and the PNIPAM was dispersed in a coil-like state below the LCST [Figure 5(b)]. More than 400 nanocapsules in TEM images (diluted in ethanol and dried at 50°C) were statistically counted to get the size and particle size distribution in dry state as shown in Figure 6. According to the formulas in the document[19] about the particle size measurement, get the mean number diameter $d_n = 59.3$ nm, mean volume diameter $d_v = 63.7$ nm and Z-average diameter $d_z = 81.2$ nm.

Figure 7 shows the schematic structure of the synthesized nanocapsule by comparing the size investigated by DLS and the size statistically calculated in the TEM images.

Tracer Diffusion Performance of Nanocapsules

Figures 8 and 9 display the time-dependent diffusion curves by monitoring the relative intensity of cresol red with UV spectroscopy, and shows the effect of solvent and temperature on the diffuse performance.

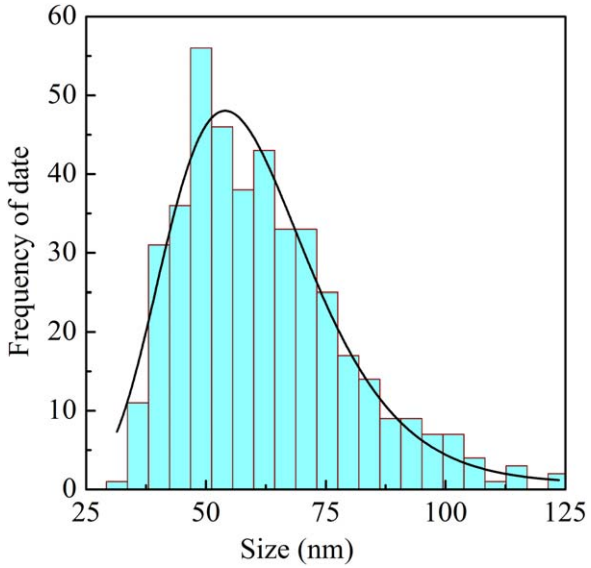

Figure 6. Size distribution of nanocapsules in TEM image. [Color figure can be viewed in the online issue, which is available at wileyonlinelibrary.com.]

Based on the Fick's law:

$$F(x,t) = -D\frac{\partial C(x,t)}{\partial x} \tag{3}$$

The diffusion flux of tracer per unit volume of shell wall is combined with the tracer concentration by function (4).

$$\frac{dC_w}{dt} = -A(C_w - C_v) \tag{4}$$

$$A = \frac{P \cdot S}{V} = \frac{3P}{R} = \frac{3D}{Rh} \tag{5}$$

where S and V are the surface area and volume of nanocapsule, P is the permeability, which can be converted into a diffusion coefficient (D) by means of multiplying the permeability with the shell wall thickness (h), $P = D/h$[20], C_w and C_v represent the concentration of tracer in solution and nanocapsules.

By integrating eq. (4), the concentration of tracer in solution becomes

$$C_w = C_0 \cdot e^{-At} \tag{6}$$

As the tracer intensity $I(t)$ depend on the concentration is theoretically described as:

$$I(t) = \phi_v n_v + \phi_w n_w \tag{7}$$

where ϕ_v and ϕ_w , represent the ultraviolet-visible absorption coefficient of tracer in the nanocapsules and solution; n_v and

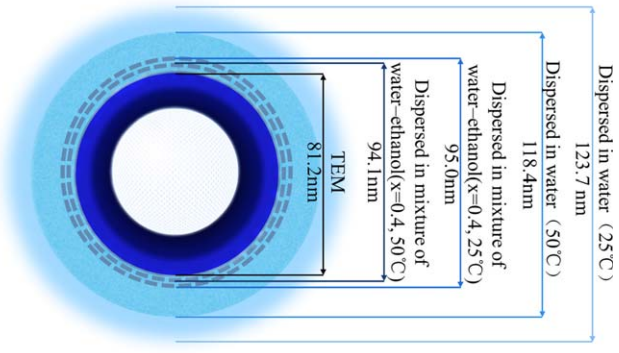

Figure 7. Structure of nanocapsules. [Color figure can be viewed in the online issue, which is available at wileyonlinelibrary.com.]

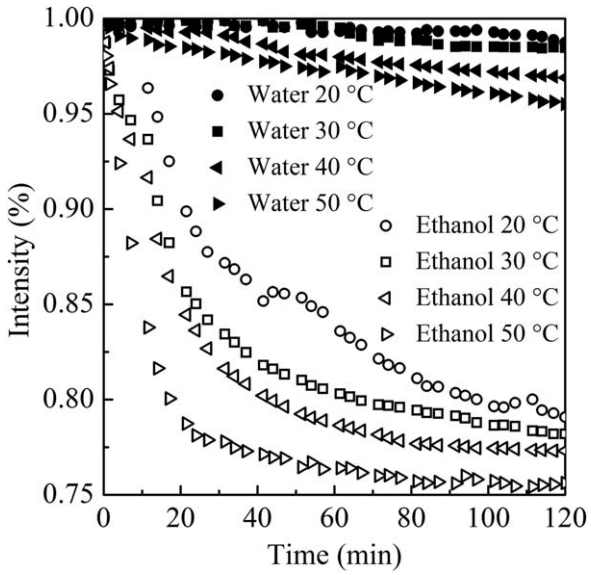

Figure 8. Time-dependent loading diffusion curves of cresol red in different medium at different temperature.

n_w are the number of tracer in the nanocapsules and solution. Thus the eq. (6) becomes $n_w = n_0 \cdot e^{-At}$. After being substituted to eq. (7), $I(t)$ can be described as

$$I(t) = \phi_v n_0 + (\phi_w - \phi_v) n_0 e^{-At}$$
$$I(t=\infty) = \phi_v n_0, \quad I(t=0) = \phi_w n_0 \tag{8}$$

And the relative intensity I_r becomes

$$I_r = \frac{I(t) - I(t=\infty)}{I(t=0) - I(t=\infty)} = e^{-At} = e^{-3Dt/Rh} \tag{9}$$

Concerning the diffusion curves, it can be expected that the time dependence of the tracer concentration is exponential.[21] Curve-fitting

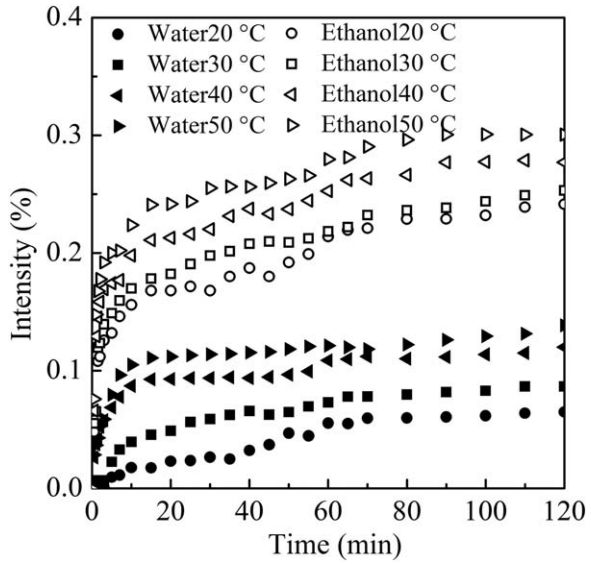

Figure 9. Time-dependent releasing diffusion curves of cresol red in different medium at different temperature.

Table III. Values of Diffusion Coefficient in Nanocapsules at Different Temperature and in Different Medium

		$D \times 10^{14}$ (cm^2/s)			
Solvent		20°C	30°C	40°C	50°C
Loading	Water	0.0041	0.133	1.27	1.46
	Ethanol	6.38	7.15	8.63	19.98
Releasing	Water	1.83	4.52	15.49	15.20
	Ethanol	57.05	57.85	85.83	87.36

calculation for the diffusion curves have been carried out and values of diffusion coefficient in nanocapsules were shown in Table III.

One clearly observes a much faster loading in ethanol than water (Figure 8). For the ethanol weakening, the hydration of polymer and driving polymer chain curled, the thickness of hydration layer reduced, as well as the particle size, thus to decrease the diffusion resistance for the tracer and opened the pathway to nanocapsules. The increase of temperature also helps to accelerate the diffusion, since it works on the thermo-sensitive polymer chain and speeds up the molecular motion. However, the effect of temperature is far less than the ethanol solvent, which can also be seen in the change of particle size. The tracer releasing curves (Figure 9) show the higher diffusion rate than the loading diffusion rate at the same condition because cresol red is water-soluble and it is easier to diffuse into water than in polymer. Comparing the releasing curves of 30and 40°C in water, it is obvious to find a sudden change signified that the temperature could control the release of cresol red, as the diffusion coefficient at 40°C is nearly four times larger than at 30°C. While the release diffusion coefficient in ethanol is about 50 times of water, it is a striking change to become a switch of nanocapsules releasing. The study shows the importance of solvent-induced interaction. And it is the main driving force of PNIPAM coil-to-globule transition for its strong influence on the hydration layer of nanocapsule.

CONCLUSION

The thermo-sensitive nanocapsules have been successfully prepared and clearly detected the hydration layer, which contains a small quantity of nonfreezing water and freezable water. The properties and content of the water in the hydration layer was proved to have a very large impact on the size and morphology of nanocapsules.

The changes of temperature and solvent can both significantly influence the structure and thickness of the hydration layer by causing the polymer chain in the shell coil-to-globule transition. Meanwhile, the thickness of the hydration layer can be controlled by the ethanol–water mixed solvent, ranging from 6.9 to 51.4 nm. That is significant to control the loading and releasing channel of nanocapsules. As the ethanol–water molecule cluster can form a rather stable associative structure around ethanol mole fraction of 0.4 and the thickness of hydration layer reached the minimum, we suggest the size under that condition would be appropriate to study other properties of latex particle. Moreover, the solvent-induced interactions were proved to be the major driving force for PNIPAM coil-to-globule transition,

which could improve the application of PNIPAM in controlled drug delivery system and phase-change materials.

ACKNOWLEDGMENTS

We thank the National Natural Science Foundation of China (NSFC) project (21176210), Outstanding Youth Foundation of Zhejiang Province (R4110199), and the Innovation Research Team of Zhejiang Province (2009R50016).

REFERENCES

1. Gu, Y.; Zhong, Y.; Meng, F.; Cheng, R.; Deng, C.; Zhong, Z. *Biomacromolecules* **2013**, *14*, 2772.
2. Landfester, K.; Musyanovych, A.; Mailänder, V. *J. Polym. Sci. Part A Polym. Chem.* **2010**, *48*, 493.
3. Ni K. F.; Shan G. R.; Weng Z. X. *CIESC J.* **2005**, *56*, 1575.
4. Chen, C.; Chen, Z.; Zeng, X.; Fang, X.; Zhang, Z. *Colloid Polym. Sci.* **2012**, *290*, 307.
5. Kumar, M.; Grzelakowski, M.; Zilles, J.; Clark, M.; Meier, W. *Proc. Natl. Acad. Sci.* **2007**, *104*, 20719.
6. Yang, Q.; Adrus, N.; Tomicki, F.; Ulbricht, M. *J. Mater. Chem.* **2011**, *21*, 2783.
7. Cao, Z. H.; Shan, G. R.; Sheibat-Othman, N.; Putaux, J. L.; Bourgeat-Lami, E. *J. Polym. Sci. Part A Polym. Chem.* **2010**, *48*, 593.
8. Cao, Z. H.; Cui, Q. M.; Shan, G. R. *Acta Polym. Sinica* **2007**, *12*, 1116.
9. Kim, Y. S.; Dong, L. M.; Hickner, M. A.; Glass, T. E.; Webb, V.; McGrath, J. E. *Macromolecules* **2003**, *36*, 6281.
10. Meersman, F.; Wang, J.; Wu, Y. Q.; Heremans, K. *Macromolecules* **2005**, *38*, 8923.
11. Hoffman, A. S. *Adv. Drug Deliv. Rev.* **2002**, *43*, 3.
12. Kumar, S.; Kim, D. W.; Lee, H. J.; Changez, M.; Yoon, T. H.; Lee, J. S. *Macromolecules* **2013**, *46*, 7166.
13. Kujawa, P.; Segui, F.; Shaban, S.; Diab, C.; Okada, Y.; Tanaka, F.; Winnik, F. M. *Macromolecules* **2006**, *39*, 341.
14. ten Wolde, P. R.; Chandler, D. *Proc. Nat. Acad. Sci. USA* **2002**, *99*, 6539.
15. Zhang, C. J.; Yang, X. N. *Fluid Phase Equil.* **2005**, *231*, 1.
16. Amo, Y.; Tominaga, Y. *Chem. Phys. Lett.* **2000**, *320*, 703.
17. Zhang, L.; Wang, Q.; Liu, Y. C.; Zhang, L. Z. *J. Chem. Phys.* **2006**, *125*, 104502.
18. Atkins, P.; De Paula, J. Physical Chemistry; Oxford University Press: New York, **2006**; Chapter 5, p 137.
19. Zhang, M. G.; Weng, Z. X.; Huang, Z. M.; Pan Z. R. *Polym. Mater. Sci. Eng.* **2000**, *16*, 1.
20. Antipov, A. A.; Sukhorukov, G. B.; Donath, E.; Möhwald, H. *J. Phys. Chem. B* **2001**, *105*, 2281.
21. Ibarz, G.; Dähne, L.; Donath, E.; Möhwald, H. *Chem. Mater.* **2002**, *14*, 4059.